Inorganic Chemistry
Article

Inorg. Chem. **2009**, *48*, 8977–8984 **8977**
DOI: 10.1021/ic900890n

Synthesis and Structure of an "Iron-Doped" Copper Selenide Cluster Molecule: $[Cu_{30}Fe_2Se_6(SePh)_{24}(dppm)_4]$

Andreas Eichhöfer,*,† Jolanta Olkowska-Oetzel,† Dieter Fenske,†,‡ Karin Fink,† Valeriu Mereacre,‡ Annie K. Powell,†,‡ and Gernot Buth§

†*Institut für Nanotechnologie, Forschungszentrum Karlsruhe, Postfach 3640, 76021 Karlsruhe, Germany,* ‡*Institut für Anorganische Chemie der Universität Engesserstrasse, Geb. 30.45, 76128 Karlsruhe, Germany, and* §*Institut für Synchrotronstrahlung (ISS), Forschungszentrum Karlsruhe GmbH, Postfach 3640, 76021 Karlsruhe, Germany*

Received May 7, 2009

CuCl and bis(diphenylphosphanyl)methane (dppm) react in the presence of small amounts of $FeCl_3$ with $PhSeSiMe_3$ and $Se(SiMe_3)_2$ to yield $[Cu_{30}Fe_2Se_6(SePh)_{24}(dppm)_4]$. The crystal structure of the compound was determined by single-crystal X-ray analysis to give a mixed copper selenide/selenolate cluster molecule of a new structural type incorporating two central iron atoms. The formal oxidation state of the iron atoms was determined by Mössbauer spectroscopy to be +3, in agreement with quantum chemical calculations and modeling of the magnetic data. In addition, Mössbauer studies show no magnetic hyperfine structure in zero field, and the magnetically perturbed spectrum displays a pattern typical for a diamagnetic species in a transverse field, suggesting a singlet ground state. However, the inclusion of the iron atoms has a distinct influence on the optical properties of the compound compared to similar clusters containing only copper and selenium atoms.

Introduction

The synthesis of ternary cluster molecules has attracted recent interest. Examples of different compounds include $(PPh_4)[Cu_6In_3(SEt)_{16}]$,[1] $[M^I{}_6M^{III}{}_8Cl_4E_{13}(PPh_3)_6]$ (M^I = Cu, Ag; M^{III} = Ga, In; E = S, Se),[2] $[Cu_{11}In_{15}Se_{16}(SePh)_{24}(PPh_3)_4]$,[3] $[Ag_{26}In_{18}S_{36}Cl_6(dppm)_{10}(thf)_4][InCl_4(thf)]_2$ (dppm = bis(diphenylphosphanyl)methane; thf = tetrahydrofuran),[4] $[Hg_{15}Cu_{20}S_{25}(PnPr_3)_{18}]$,[5,6] $[Cu_4Nb_2Se_6(PMe_3)_8]$,[7] $[Ta_4Cu_{12}Cl_8S_{12}(PMe_3)_{12}]$,[8] $[(N,N'\text{-tmeda})_5Zn_5Cd_{11}Se_{13}(SePh)_6(thf)_2]$,[9] and $[(py)_8Ln_4M_2Se_6(SePh)_4]$ (Ln = Er, Yb, Lu; M = Cd, Hg).[10] In addition to the structural characterization of such compounds, the investigation of properties relevant to their potential use as precursor materials for photovoltaic materials[1,11] and their fluorescence properties[9,10] are of interest. These are dependent on the elements present and their relative ratio, the size of the cluster, and also the nature of the ligands. In this context, to date, only a limited number of cluster compounds have been synthesized comprising copper, iron, and sulfur or selenium, for example, $[Fe_3Cu(SiPr)_6Cl_3]^{2-}$,[12] $[Fe_2Cu_4(SiPr)_8Cl_3]^{2-}$,[13] $[Cu_4Fe_4S_6(PnPr_3)_4Cl_4]$, $[Cu_2Fe_6S_6(PEt_3)_2Cl_6](Bu_4N)_2$,[14] $[Cu_5Fe(SePh)_7(PPh_3)_4]$, and $[Cu_4Fe_3(SePh)_{10}(PPh_3)_4]$,[15] which should also be interesting to study with respect to their magnetic properties.

*To whom correspondence should be addressed. Tel.: +7247-82-6371. Fax: +7247-82-6368. E-mail: eichhoefer@int.fzk.de.

(1) Hirpo, W.; Dhingra, S.; Kanatzidis, M. *J. Chem. Soc., Chem. Comm.* **1992**, 557–559.
(2) Olkowska-Oetzel, J.; Fenske, D.; Scheer, P.; Eichhöfer, A. *Z. Anorg. Allg. Chem.* **2003**, *629*, 415–420.
(3) Eichhöfer, A.; Fenske, D. *J. Chem. Soc., Dalton Trans.* **2000**, 941–944.
(4) Ahlrichs, R.; Eichhöfer, A.; Fenske, D.; Hampe, O.; Kappes, M. M.; Nava, P.; Olkowska-Oetzel, J. *Angew. Chem.* **2004**, *116*, 3911–3915. Ahlrichs, R.; Eichhöfer, A.; Fenske, D.; Hampe, O.; Kappes, M. M.; Nava, P.; Olkowska-Oetzel, J. *Angew. Chem., Int. Ed.* **2004**, *43*, 3823–3827.
(5) Tran, D. T. T.; Beltran, L. M. C.; Kowalchuk, C. M.; Trefiak, N. R.; Taylor, N. J.; Corrigan, J. F. *Inorg. Chem.* **2002**, *41*, 5693–5698.
(6) Tran, D. T. T.; Taylor, N. J.; Corrigan, J. F. *Angew. Chem.* **2000**, *112*, 965–967. Tran, D. T. T.; Taylor, N. J.; Corrigan, J. F. *Angew. Chem., Int. Ed.* **2000**, *39*, 935–937.
(7) Lorenz, A.; Fenske, D. *Angew. Chem.* **2001**, *113*, 4537–4541. Lorenz, A.; Fenske, D. *Angew. Chem., Int. Ed.* **2001**, *40*, 4402. Lorenz, A.; Fenske, D. *Z. Anorg. Allg. Chem.* **2001**, *627*, 2232–2248.
(8) Pätow, R.; Fenske, D. *Z. Anorg. Allg. Chem.* **2002**, *628*, 1279–1288.
(9) DeGroot, M. W.; Taylor, N. J.; Corrigan, J. F. *J. Am. Chem. Soc.* **2003**, *125*(4), 864–865.
(10) Kornienko, A.; Banerjee, S.; Kumar, G. A.; Riman, R. E.; Emge, T. J.; Brennan, J. G. *J. Am. Chem. Soc.* **2005**, *127*, 14008–14014.
(11) Hirpo, W.; Dhingra, S.; Sutorik, A. C.; Kanatzidis, M. *J. Am. Chem. Soc.* **1993**, *115*, 1597–1599.
(12) Stephan, H.-O.; Henkel, G.; Kanatzidis, M. G. *Chem. Commun.* **1997**, 67–68.
(13) Lackmann, J.; Hauptmann, R.; Weissgräber, S; Henkel, G. *Chem. Commun.* **1999**, 1995–1996.
(14) Koutmos, M.; Kalyvas, H.; Sanakis, Y.; Simopoulos, A.; Coucouvanis, D. *J. Am. Chem. Soc.* **2005**, *11*, 3706–3707.
(15) Eichhöfer, A.; Fenske, D.; Olkowska-Oetzel, J. *Eur. J. Inorg. Chem.* **2007**, 74–79.

Published on Web 08/19/2009

Table 1. Crystallographic Data for $[Cu_{30}Fe_2Se_6(SePh)_{24}(dppm)_4]$ (**1**)

	$\mathbf{1}\cdot 9C_4H_8O$
fw [g/mol]	8423.50
cryst syst	monoclinic
space group	$P2_1/c$
a [pm]	2220.8(4)
b	2826.0(6)
c	2469.1(5)
α [deg]	
β	105.67(3)
γ	
V [10^9pm^3]	14920(5)
Z	2
T [K]	180
d_{calcd} [g cm^{-3}]	1.875
$\mu(\lambda)$ [mm^{-1}]	5.934 (Mo Kα)
F[000]	8188
$2\theta_{max}$ [deg]	44
measd reflns	42156
unique reflns	17755
R_{int}	0.0664
reflns with $I > 2\sigma(I)$	10189
refined params	1521
R1 ($I > 2\sigma(I)$)[a]	0.0540
wR2 (all data)[b]	0.1430

[a] $R1 = \sum||F_o| - |F_c||/\sum|F_o|$. [b] $wR2 = \{\sum[w(F_o^2 - F_c^2)^2]/\sum[w(F_o^2)^2]\}^{1/2}$.

Herein, we report the synthesis and characterization of a mixed copper selenide/selenolate cluster molecule $[Cu_{30}Fe_2Se_6(SePh)_{24}(dppm)_4]$ of a new structural type incorporating two central iron atoms.

Results and Discussion

The reaction of CuCl and 0.07 equiv of $FeCl_3$ with $PhSeSiMe_3$ and $Se(SiMe_3)_2$ in the presence of dppm yielded black crystals of **1** (eq 1).

$$\mathrm{CuCl} + 0.07\mathrm{FeCl_3} + 0.2\mathrm{dppm} \xrightarrow[\mathrm{THF}]{+1.5\mathrm{PhSeSiMe_3}/0.2\mathrm{Se(SiMe_3)_2}} [\mathrm{Cu_{30}Fe_2Se_6(SePh)_{24}(dppm)_4}] \quad (1)$$

Crystal Structure. Compound **1** crystallizes in the monoclinic space group $P2_1/c$ with the molecules residing on a center of inversion symmetry (Table 1). The selenium atoms of the selenido ligands (Se1, Se1′, Se2, Se2′, Se3, and Se3′) and the phenyl-selenolato ligands (Se4−Se30 and symmetry equivalent positions) form a three-layered distorted cubic close-packed network with nonbonding distances ranging from 349.6 to 440.9 pm (Figure 1b). The 32 metal atoms partially occupy tetrahedral holes within the network or else are found at distorted trigonal sites on the surface of the cluster (Figure 1a). Assuming that the selenido ligands carry a formal charge of −2 and the phenylselenolato ligands carry a single negative charge, the 32 metal atoms should carry a total of 36 positive charges in order to preserve charge balance for the cluster. This leads to three possible combinations of metal valencies also allowing for the possibility that no iron is included in the core, namely, (a) 28 Cu^{1+} and 4 Cu^{2+} ions with no iron present, (b) 28 Cu^{1+} and 4 Fe^{2+} ions, and (c) 30 Cu^{1+} and 2 Fe^{3+} ions. Scenario a, with exclusively copper atoms at the metal sites, is the most unlikely since reactions carried out omitting the iron salt did not yield crystals at all and none of the metal coordination sites correspond to arrangements typical for the Cu^{2+} ion.

Instead, two iron atoms were found to occupy the two tetrahedral coordination sites formed by the six selenido ligands in the center of **1**. The inclusion of iron atoms in the crystals was proven by fluorescence X-ray absorption near edge spectroscopy (XANES) of a single crystal of **1** at the ANKA synchrotron source. The spectrum exhibits a marked shoulder in the steeply rising absorption edge region that is characteristic for tetrahedrally coordinated iron (Figure 2).[16] In addition, the energetic position, energy splitting, and intensity distribution of the pre-edge features in the region of the 1s → 3d transition have been shown in previous investigations to be sensitive to the spin state, oxidation state, geometry, and bridging ligation of iron atoms.[17,18] Complex **1** displays a relatively intense single pre-edge feature, as expected for tetrahedrally coordinated ferric atoms, where the transition can gain intensity both through an allowed electric quadrupole mechanism and from an electric dipole mechanism associated with 4p mixing into 3d orbitals. However, the peak is not as well separated from the onset of the mean absorption feature, as observed for monomeric $(NEt_4)[FeCl_4]$ and dimeric $(BzPhMe_2N)_2[Fe_2OCl_6]$.[17] In view of the difficulty to find XANES data of comparable tetrahedral coordinated Fe−Se molecular complexes in the literature, we measured the spectrum of a divalent reference compound, $[Cu_5Fe(SePh)_7(PPh_3)_4]$,[15] which comprises a tetrahedrally coordinated ferrous ion. The pre-edge feature of this compound appears to be broader than that of **1** but is not split into two peaks as expected and observed for tetrahedral coordinated ferrous complexes $(NEt_4)_2[FeCl_4]$, Cs_3FeCl_5, and $Fe(HB(3,5\text{-}i\mathrm{Pr}_2\mathrm{pz})_3)Cl$.[17] The energy position of the pre-edge peak in **1** is approximately 0.5 eV above the pre-edge peak of $[Cu_5Fe(SePh)_7(PPh_3)_4]$. This trend is in agreement with observations on the above-mentioned tetrahedral coordinated complexes where the ferric pre-edge features in $(NEt_4)[FeCl_4]$ and dimeric $(BzPhMe_2N)_2[Fe_2OCl_6]$ are centered at ∼0.8 eV higher energy (∼7113.3 eV) than their ferrous counterparts $(NEt_4)_2[FeCl_4]$, Cs_3FeCl_5, and $Fe(HB(3,5\text{-}i\mathrm{Pr}_2\mathrm{pz})_3)Cl$ (∼7112.4 eV). An interrelation concerning the difference in energy position of the pre-edge feature between ferric and ferrous iron atoms was also observed for octahedral coordinated high-spin iron complexes.[17] However, the obtained XANES data appear to be insufficient to derive the formal oxidation state of the two iron atoms in **1**.

The X-ray structure analysis carried out at the ANKA synchrotron source at a wavelength close to the absorption edge of copper of 1.38 Å gave, as a result of the enlarged differences in the atomic form factors of copper and iron, reasonable thermal displacement parameters only for the atom assignment shown in Figure 1a). Fe−Se distances range from 241.1(2) (Se1−Fe1′) to 243.2(2) (Se2−Fe1) pm and Se−Fe−Se angles from 102.55(8) (Se1′−Fe1−Se3) to 113.81(8) (Se1′−Fe1−Se2), comparable to values found for four-coordinated iron atoms in $[Fe_4Se_4(SeMe)_4]^{2-}$ (Fe−Se, 237.0−243.6 pm; Se−Fe−Se, 104.84−116.22°).[19]

(16) Manceau, A.; Gates, W. P. *Clays Clay Miner.* **1997**, *45*(3), 448–460.
(17) Westre, T. E; Kennepohl, P.; DeWitt, J. G.; Hedman, B.; Hodgson, K. O.; Solomon, E. I. *J. Am. Chem. Soc.* **1997**, *119*, 6297 –6314.
(18) Shulman, R. G.; Yafet, Y.; Eisenberger, P.; Blumberg, W. E. *Proc. Natl. Acad. Sci. U. S. A.* **1976**, *73*, 1384.
(19) Kern, A.; Näther, Ch.; Studt, F.; Tuczeck, F. *Inorg. Chem.* **2004**, *43* (16), 5003–5010.

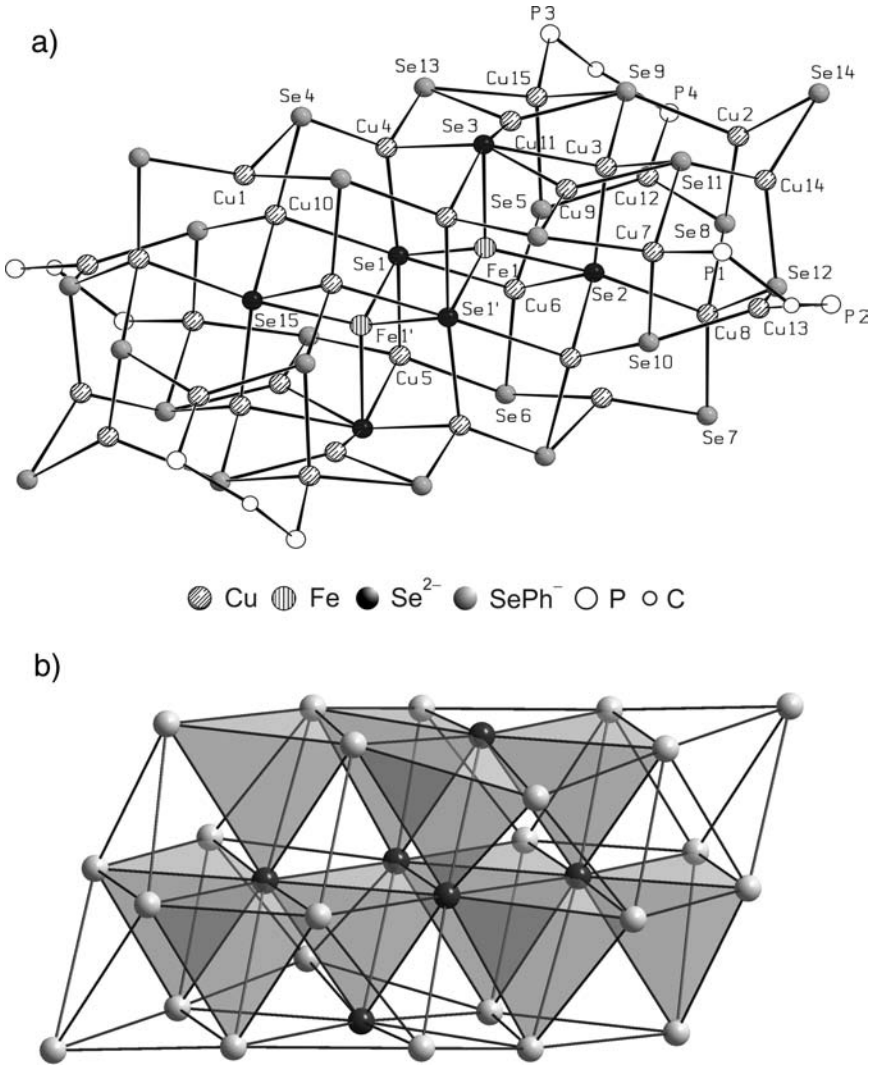

Figure 1. (a) Molecular structure of the cluster $[Cu_{30}Fe_2Se_6(SePh)_{24}(dppm)_4]$ (**1**). C and H atoms are omitted for clarity. Selected bond lengths [pm] and angles [deg]: Se(1)−Fe(1)′, 241.1(2); Se(1)−Fe(1), 242.7(2); Se(1)′−Fe(1)−Se(3), 106.82(8); Se(1)′−Fe(1)−Se(1), 102.55(8); Se(3)−Fe(1)−Se(1), 108.88(8); Se(1)′−Fe(1)−Se(2), 113.81(8); Se(3)−Fe(1)−Se(2), 110.87(9); Se(1)−Fe(1)−Se(2), 113.38(8). Nonbonding distance Fe1···Fe1′, 302.7(2). (b) Substructure of the selenium atoms in **1**. Range of nonbonding Se−Se distances: 349.6−440.9 pm.

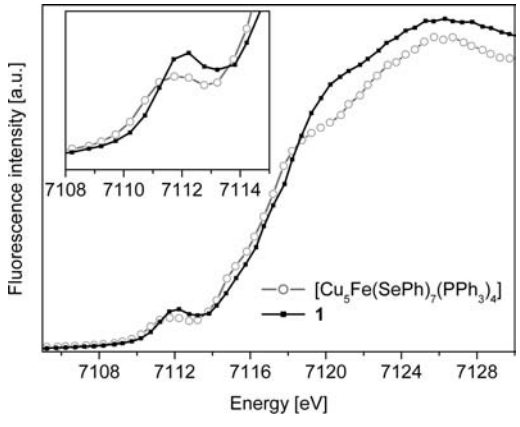

Figure 2. Fluorescence XANES spectra of $[Cu_{30}Fe_2Se_6(SePh)_{24}(dppm)_4]$ (**1**) (black squares) and $[Cu_5Fe(SePh)_7(PPh_3)_4]$ (gray circles). The inset shows the pre-edge peak region.

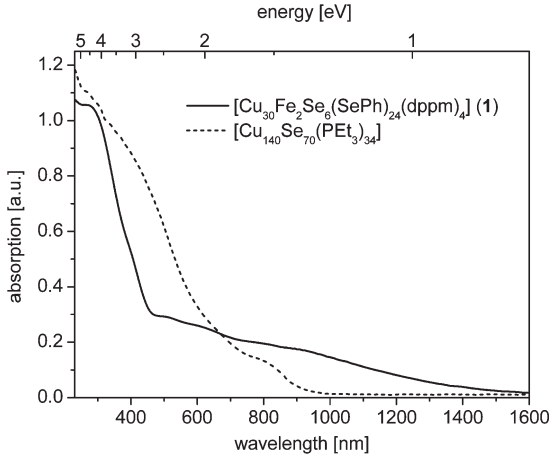

Figure 3. UV−vis spectra of $[Cu_{30}Fe_2Se_6(SePh)_{24}(dppm)_4]$ (**1**) as a mull in nujol (straight line) compared with that of $[Cu_{146}Se_{73}(PEt_3)_{34}]$ (dashed line).

This central dinuclear Fe_2Se_6 unit is surrounded by a distorted cubic network formed by the 24 phenylselenolate surface ligands and the 30 copper atoms. Assuming an upper limit of 300 pm for Cu−Se bonding interactions, the copper atoms (Cu1−Cu11, Cu14, and symmetry equivalent positions) which are solely coordinated by selenium atoms adopt a range of distorted coordination modes from

Table 2. TDDFT Transition Energies [eV] and Wavelengths [nm] (in brackets) Calculated for Two Model Complexes and $[Cu_{30}Fe_2Se_6(SePh)_{24}(dppm)_4]$ (**1**)

	model 1		model 2		**1**
	$[M_2Se_6]^{6-}$		$[Cu_{30}M_2Se_6(SeCH_3)_{24}(PH_3)_8]$		$[Cu_{30}Fe_2Se_6(SePh)_{24}(dppm)_4]$
	M = Fe	M = Al	M = Fe	M = Al	
BP86 eV (nm)	1.29 (961)	4.90 (253)	0.70 (1771)	1.59 (782)	0.71 (1744)
B3-LYP eV (nm)	1.94 (637)	5.47 (226)			
transition	Se → Fe(3d)	Se → Al	CuSe → Fe(3d)	CuSe → CuL	CuSe → Fe(3d)

Table 3. The Mössbauer Spectral Parameters for $[Cu_{30}Fe_2Se_6(SePh)_{24}(dppm)_4]$ (**1**)

T, K	δ^a, mm/s	ΔE_Q, mm/s	Γ, mm/s
294	0.445(5)	0.386(7)	0.37(1)
200	0.507(4)	0.415(6)	0.43(1)
77	0.571(4)	0.467(6)	0.441(1)
3	0.584(2)	0.461(4)	0.447(6)

[a] Relative to α-Fe at room temperature.

a slightly distorted tetrahedral arrangement for Cu6 (Cu−Se, 240.8−265.5(2) pm; Se−Cu−Se, 103.77−116.82(8)°) to an almost trigonal planar coordination for Cu11 (Cu−Se, 241.8(2)−248.1(2) pm; Se−Cu−Se, 117.70(8)−119.54(9)°).

The four bidentate bis(diphenylphosphanyl)methane ligands occupy four edges of the rectangular $\{Cu_{30}Fe_2Se_{36}\}$ cluster core, each with one of the phosphorus atoms bonded to a three-coordinated copper atom (Cu12, Cu12′, Cu13, Cu13′) and the other bonded to a four-coordinated copper atom (Cu7, Cu7′, Cu15, Cu15′) with Cu−P distances ranging from 219.7(4) (Cu13−P2) to 225.3 (Cu15−P3) pm.

Electronic Properties. UV−vis spectra of the black crystals of **1** measured as a nujol mull pressed between quartz plates display a continuous and featureless increase of the absorption in the region between 1600 and 460 nm (Figure 3). After this, the absorption increases significantly to show a maximum around 270 nm, which can most probably be assigned to transitions within the $SePh^-$ and dppm ligands. It is interesting to note that the onset of absorption is significantly shifted to a higher wavelength compared with that of one of the largest copper selenide clusters known, $[Cu_{140}Se_{70}(PEt_3)_{34}]$,[20] which suggests that the incorporation of two iron atoms in the copper selenide cluster has a distinct influence on its electronic properties.

We analyzed the influence of the Fe centers in **1** on the optical spectra by time-dependent density functional theory (TDDFT). The lowest electronic transitions for three different models are given in Table 2 (model 1, $[Fe_2Se_6]^{6-}$ embedded in a point charge field; model 2, $[Cu_{30}Fe_2Se_6(SeCH_3)_{24}(PH_3)_8]$; and **1**; for details, see the Experimetal Section). Hence, for model 2 and **1**, the low energy transitions can be characterized as a charge transfer from the CuSe cluster framework into singly occupied 3d orbitals of the Fe ions. In calculations on a compound where Fe was substituted by Al, the lowest transitions are 0.89 eV higher in energy, which is in good agreement with the experimentally observed shift of **1** with respect to pure copper selenide clusters. In a simple dimeric $[Fe_2Se_6]^{6-}$ model compound, the lowest transitions are shifted by 0.59 eV to higher energy in comparison to **1**.

Mössbauer Spectra. If one assumes formal charges of +1 for the copper atoms (Cu^+), −2 for the selenido ligands (Se^{2-}), and −1 for the selenolato ligands ($SePh^-$), the two iron atoms should carry two formal +3 charges. However, it is also possible that Fe^{3+} is reduced to Fe^{2+} in the presence of Cu^+ in order to yield a delocalized mixed-valent Cu^+/Cu^{2+} network, which might also explain the unusual optical properties of **1**. According to the values of reduction potentials in aqueous media, the Cu^+/Fe^{3+} should be stable under basic (pH = 14) conditions, while at pH = 0, the redox potentials suggest Fe^{2+}/Cu^{2+} should be stable. In order to identify the charge states of the two iron atoms at the center of **1**, Mössbauer spectra were measured on samples synthesized with 50% ^{57}Fe-enriched $FeCl_3$.

The Mössbauer spectra of **1** were measured between 3 and 294 K and fit with a single quadrupole doublet. The resulting spectral hyperfine parameters are given in Table 3, and selected spectra are shown in Figure 4. It should be noted that Mössbauer data for synthetic 2Fe−2Se compounds with purely selenido bridging ligation are still quite rare.[21,22] All of the spectra are clearly indicative of high-spin iron(III) in the sort of distorted tetrahedral coordination environment found in **1**, and there is no indication of the presence of any iron(II) species (Figure 4a). The temperature dependence of the isomer shift results from the second-order Doppler shift arising from the differences between the source and absorber temperature. The increase in the values of quadrupole splitting with decreasing temperature could result either from small changes in the coordination geometry at lower temperatures or from different signs and temperature dependencies of the valence and lattice contributions to the electric field gradient experienced by the iron(III) ion in **1**. The expected increase in the spectral absorption area between 294 and 3 K results from the increase in the recoil-free fraction upon cooling. This compound shows no indication of ordering at 3 K. Its 5.0 T spectrum (Figure 4b) at 3 K exhibits a pattern typical of a diamagnetic complex measured in a perpendicular applied magnetic field. The observed magnetic Mössbauer spectrum has a magnetic splitting which is only due to the external magnetic field H_0, confirming the presence of a diamagnetic ground state, $S = 0$, as deduced from the magnetic susceptibility measurements. In other words, there is no detectable contribution from magnetic hyperfine interaction other than the applied field and therefore no residual paramagnetism at 3 K. This is likely because Cu(I) cations have a d^{10} configuration, and no transferred

(20) Zhu, N.; Fenske, D. *J. Chem. Soc., Dalton Trans.* **1999**, 1067–1075.

(21) You, J. F.; Papaefthymiou, G. C.; Holm, R. H. *J. Am. Chem. Soc.* **1992**, *114*, 2697–2710.

(22) Yu, S. B; Papaefthymiou, G. C.; Holm, R. H. *Inorg. Chem.* **1991**, *18*, 3476–3485.

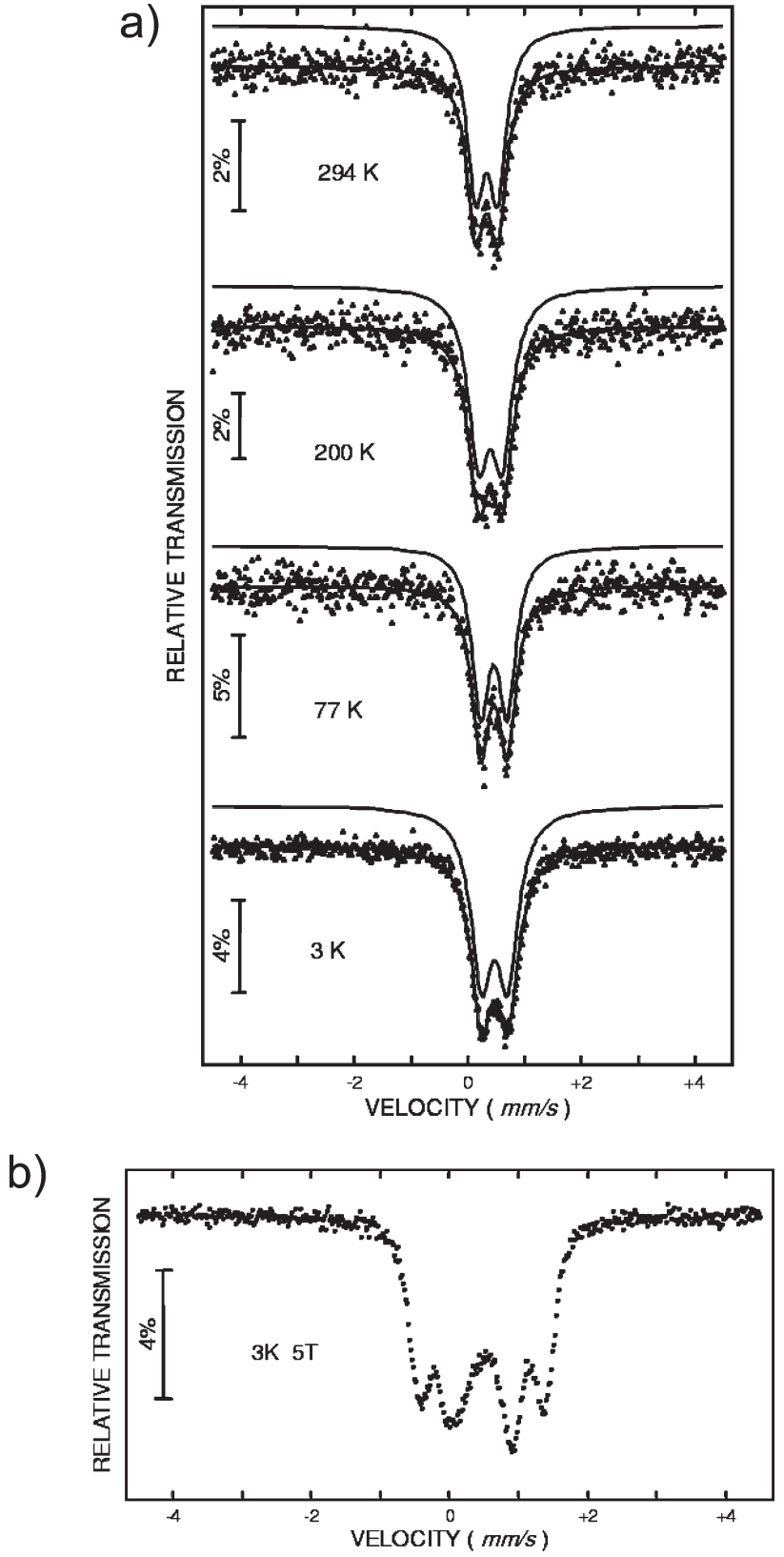

Figure 4. (a) Mössbauer spectra of $[Cu_{30}Fe_2Se_6(SePh)_{24}(dppm)_4]$ (**1**) obtained at the indicated temperatures. (b) The 3 K Mössbauer spectrum of polycrystalline **1** recorded in a perpendicular applied field of 5.0 T.

hyperfine field from the surrounding copper spins to the strongly antiferromagnetically coupled Fe(III) is expected.

Magnetic Data and Quantum Chemical Calculations. The temperature dependence of the susceptibility of **1** was measured in a field of 1 T (Figure 5a). The large diamagnetic contribution of the copper selenide cluster framework with the organic ligands was estimated from Pascal's constants to add up to a diamagnetic correction

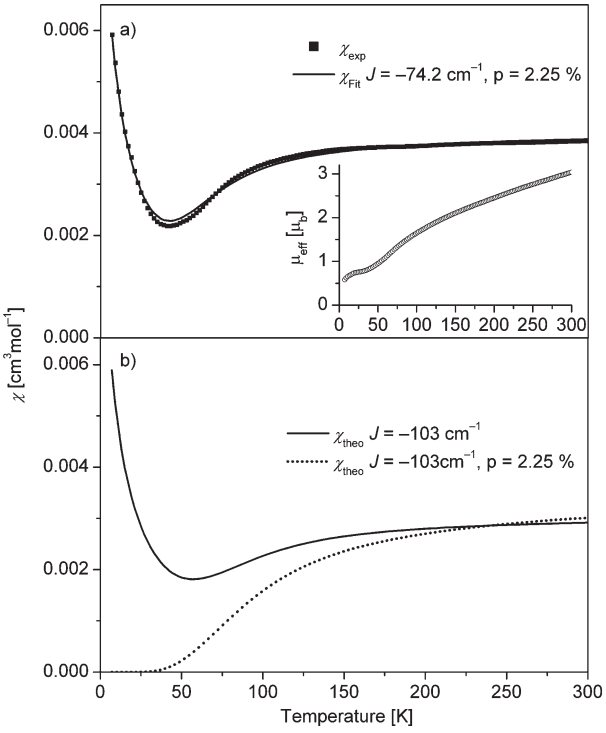

Figure 5. (a) χ_{exp} vs T plot measured at 1 T of $[Cu_{30}Fe_2Se_6(SePh)_{24}(dppm)_4]$ (**1**) (inset displays μ_{eff} vs T). The straight line represents the best fit of χ according to eq 1 with the values $J = -74.2\ cm^{-1}$ and $g = 1.88$ and considering a paramagnetic impurity by eq 2 with $S = 5/2$, $p = 2.25\%$, and $\Theta_w = -9.72$ K. (b) χ vs T plots for the quantum chemically calculated exchange coupling constant of **1** (Table 3) and $g = 1.88$ according to eq 1 (dotted lines) and considering additionally the paramagnetic impurity with the same values as in part a (straight line).

of $-0.003\ cm^3\ mol^{-1}$, which was subtracted from the data. Thus, the magnetic moment μ_{eff} at room temperature was found to be 3.2 μ_B, which is much lower than expected for two uncoupled ferric ions ($S = 5/2$). The continuous decrease of μ_{eff} upon lowering the temperature is characteristic for antiferromagnetic coupling between the two iron atoms to give an $S = 0$ ground state, as is usually observed for dinuclear [2Fe−2S] clusters.[23] The graph of χ versus T shows nearly constant susceptibility in the region from 300 to 150 K, which thereafter decreases smoothly on going to lower temperatures. From 41 K down to 7 K, the susceptibility increases again. The magnetic susceptibility data were fitted to a Heisenberg−Dirac−van Vleck Hamiltonian (eq 1) allowing for a small amount of a paramagnetic impurity (eq 2). The best fit was obtained with an exchange coupling constant $J = -74.2\ cm^{-1}$, $g = 1.88$, and a paramagnetic impurity of 2.25% with $S = 5/2$ and $\theta_W = -9.72$ K. In a series of related sulfur bridged compounds with the general formula $[Fe_2S_2(SR)_2]$ (R = organic group),[23] which comprise tetrahedrally coordinated iron atoms, similar low g values were reported, while the J values were found to be higher ($-149\ cm^{-1}$ to $-204\ cm^{-1}$). The antiferromagnetic coupling of the two iron(III) ions was also predicted from the quantum chemical calculations. The results for the magnetic exchange coupling constants of the quantum chemical calculations are summarized in Table 4.

(23) Ballmann, J.; Dechert, S.; Bill, E.; Ryde, U.; Meyer, F. *Inorg. Chem.* **2008**, *47*(5), 1586–1596.

Table 4. Calculated Exchange Coupling Constants J in cm^{-1}

	model 1 $[Fe_2Se_6]^{6-}$	model 2 $[Cu_{30}Fe_2Se_6(SeCH_3)_{24}(PH_3)_8]$	**1** $[Cu_{30}Fe_2Se_6(SePh)_{24}(dppm)_4]$
mod. CASCI	−105		
B3LYP	−146	−97	−103
BP86	−226	−148	−160
J_{BP86}/J_{B3LYP}	1.54	1.51	1.55

We performed calculations on model compounds of different sizes and with two different methods (see Experimental Section), and in all cases antiferromagnetic coupling of the two iron(III) ions was observed. This is in agreement with results obtained for iron in similar environments in sulfur-bridged iron(III) complexes.[24−26] Compared to the dimeric model 1, the consideration of the CuSe framework in model 2 reduces the exchange coupling constant from $J = -146\ cm^{-1}$ (model 1, B3LYP) to $J = -97\ cm^{-1}$ (model 2, B3LYP), while the substitution of the CH_3 groups in model 2 by external phenyl rings in **1** did not influence the coupling constant ($J = -103\ cm^{-1}$, B3LYP). In Figure 5, the quantum chemically calculated susceptibility for **1** is compared with the experimental data. The increase at low temperatures can only be explained by a small amount of a paramagnetic impurity which was estimated from the fit of the experimental data and additionally included in the quantum chemically calculated susceptibility.

Conclusion

An unusual example of an "iron-doped" copper selenide cluster molecule was synthesized and structurally characterized. The inclusion of the iron atoms has a distinct influence on the optical properties of the compound compared with similar copper selenide clusters with an absorption onset at a comparatively high wavelength. However, the charges on the metal centers seem to be localized, as Mössbauer spectra proved a charge state of +3 for the two iron atoms. Magnetic data show the expected strong antiferromagnetic coupling of the two ferric ions bridged by the selenide ligands, which could be successfully modeled by quantum chemical calculations.

Experimental Section

Synthesis. Standard Schlenk techniques were employed throughout the syntheses using a double manifold vacuum line (10^{-3} mbar) with high-purity nitrogen (99.99990%). Tetrahydrofuran was dried over sodium−benzophenone and distilled under nitrogen. CuCl was subsequently washed with HCl, CH_3OH, and diethylether to remove traces of $CuCl_2$ and dried under a vacuum. $FeCl_3$ and dppm were obtained from Aldrich. $PhSeSiMe_3$[27] and $Se(SiMe_3)_2$[28] were prepared according to literature procedures.

$[Cu_{30}Fe_2Se_6(SePh)_{24}(dppm)_4]$ (1). CuCl (100 mg, 1.01 mmol), $FeCl_3$ (11 mg, 0.067 mmol), and dppm (78 mg, 0.20 mmol) were suspended in 35 mL of thf. After 2 h of stirring, $PhSeSiMe_3$ (0.29 mL, 1.52 mmol) was added, resulting in the formation of an orange-red solution. After one night of stirring, $Se(SiMe_3)_2$

(24) Hübner, O.; Sauer, J. *Phys. Chem. Chem. Phys.* **2002**, *4*, 5234–5243.
(25) Schreiner, E.; Nair, N. N.; Pollet, R.; Staemmler, V.; Marx, D. *Proc. Natl. Acad. Sci. U. S. A.* **2007**, *104*, 20725–20725.
(26) Nair, N. N.; Schreiner, E.; Pollet, R.; Staemmler, V.; Marx, D. *J. Chem. Theory Comput.* **2008**, *4*, 1174–1188.
(27) Miyoshi, N.; Ishii, H.; Kondo, K.; Mui, S.; Sonoda, N. *Synthesis* **1979**, 301–304.
(28) Schmidt, H.; Ruf, H. *Z. Anorg. Allg. Chem.* **1963**, *321*, 270–273.

(0.045 mL, 0.2 mmol) was added to the red solution at 0 °C and the flask stored for one additional night in the refrigerator at 4 °C. The reaction solution gradually turned darker to give a black solution after one night. The mixture was then allowed to warm up to room temperature with first black crystals of **1** forming after three days. After 2 weeks, the crystals were filtered and washed two times with thf to give a total yield of 96 mg (37% with respect to Cu) of a black microcrystalline powder of **1**. The crystals are not soluble, even in polar organic solvents like thf and CH_3CN, and show only poor solubility in N,N-dimethylformamide under the formation of a brown solution and a precipitate most probably due to decomposition. Compound **1** is sensitive against oxidation and hydrolysis. Anal. Calcd for $C_{244}H_{208}Cu_{30}Fe_2P_8Se_{30}$ (**1**) (7775.0): Cu, 24.5; Fe, 1.4; Se, 30.5; C, 37.7; H, 2.7%. Found: Cu, 24.2; Fe, 1.5; Se, 30.0; C, 37.8; H, 2.7%.

Crystallography. Crystals suitable for single-crystal X-ray diffraction were taken directly from the reaction solution of the compound and then selected in perfluoroalkylether oil.

Single-crystal X-ray diffraction data of **1** were collected using graphite-monochromatized Mo Kα radiation (λ = 0.71073 Å) on a STOE IPDS II (imaging plate diffraction system). In addition, single-crystal X-ray diffraction data of **1** were also collected using synchrotron radiation (λ = 1.38061 Å) on a STOE IPDS II at the ANKA synchrotron source in Karlsruhe, Germany. The structures were solved with the direct methods program SHELXS[29] of the SHELXTL PC suite of programs and were refined with the use of the full-matrix least-squares program SHELXL.[29] Molecular diagrams were prepared using SCHAKAL 97[30] and Diamond 2.1.[31]

All Cu, Fe, Se, P, and C atoms of the cluster molecules were refined with anisotropic displacement parameters with the exception of the C and O atoms of the solvent thf molecules, which were refined isotropically. H atoms were calculated in fixed positions for the organic groups of the cluster molecule. Remaining electron density peaks indicated further disordered thf molecules which could not be refined with a satisfactory model. Most probably due to the large amount of solvent molecules incorporated in the crystal lattice, the crystals diffract only up to 2Θ 44°. A numerical absorption correction was applied.[32]

CCDC-702865 (**1**) contains the supplementary crystallographic data for this paper. These data can be obtained free of charge at www.ccdc.cam.ac.uk/conts/retrieving.html (or from the Cambridge Crystallographic Data Centre, 12 Union Road, Cambridge CB2 1EZ, UK; fax (internat.): +44−1223/336−033; e-mail: deposit@ccdc.cam.ac.uk).

Physical Measurements. C and H elemental analyses were performed on an Elementar Vario Micro Cube instrument. Cu, Fe, and Se analyses were performed by the Mikroanalytisches Labor Pascher, Remagen-Bandorf, Germany, using inductively coupled plasma atomic emission spectroscopy.

The iron X-ray fluorescence spectrum was measured by taking energy spectra of the sample crystal fluorescence with a silicon drift detector (KETEK SDD) built into the STOE IPDS II for different energy settings of the double-crystal monochromator of the ANKA SCD beamline. The photon counts within a region of interest around the Fe Kα emission lines were extracted from the spectra and normalized to the incoming photon flux.

UV−vis absorption spectra of cluster molecules in the solid state were measured on a Varian Cary 500 spectrophotometer as a nujol mull sandwiched between quartz plates using a Labsphere integrating sphere.

Temperature-dependent DC susceptibilities were recorded on a Quantum Design MPMS-5S SQUID magnetometer in RSO mode on powdered samples which were loaded into gelatin capsules in a glovebox.

The Mössbauer spectra were acquired using a conventional spectrometer in the constant-acceleration mode equipped with a ^{57}Co source (3.7 GBq) in a rhodium matrix. Isomer shifts are given relative to α-Fe at room temperature. The sample was inserted inside an Oxford Instruments Mössbauer-Spectromag 4000 Cryostat, which has a split-pair superconducting magnet system for applied fields up to 5 T, with the field of the sample oriented perpendicular to the γ-ray direction, while the sample temperature can be varied between 3.0 and 300 K. The zero-field spectra were fitted using the NORMOS Mössbauer fitting program.

Quantum Chemical Calculations. Optical transitions and the magnetic exchange coupling were obtained for model compounds of different sizes, making it possible to investigate the influence of the inclusion of the magnetic atoms in the CuSe cluster framework as well as the influence of the terminal ligands on the electronic structure. In model 1, only the $[Fe_2Se_6]^{6-}$ core of the compound was described fully quantum mechanically. The Cu atoms were substituted by a positive charge and a pseudo potential and the Se atoms by point charges with the charge −1. In model 2, the $Cu_{30}Fe_2Se_{30}$ cluster core was completely taken into account, while the phenyl ligands were substituted by CH_3 groups and each dppm ligand by two PH_3 groups. Finally, we also performed calculations on **1**. In all calculations, the geometry of the $\{Cu_{30}Fe_2Se_{30}\}$ core of the molecule was taken from the X-ray diffraction structure, while the positions of the ligand atoms were optimized by DFT calculations using the BP86 functional for model 2 and by a force field calculation for **1**.

To judge whether the red shift of the absorption onset is a result of the unpaired electrons of the Fe(III) atoms, TDDFT calculations were performed for the different models and the analogues in which paramagnetic Fe(III) was replaced by diamagnetic Al(III).

The exchange coupling constants were obtained using two different methods. On the one hand, DFT calculations in the framework of the broken symmetry approach[33,34] were applied. The exchange coupling constants were obtained by the spin-projected method of Yamaguchi and co-workers.[34,35]

$$J = \frac{E(\mathrm{BS}) - E(\mathrm{HS})}{\langle S^2\rangle_{\mathrm{HS}} - \langle S^2\rangle_{\mathrm{BS}}}$$

Additionally, we used the modified CASCI method.[36]

All DFT and TDDFT calculations were performed with the program package Turbomole.[37−41] The exchange coupling constants were obtained with two different functionals, BP86[42,43]

(29) Sheldrick, G. M. *SHELXTL PC*, version 5.1; Bruker Analytical X-ray Systems: Karlsruhe, Germany, 2000.
(30) Keller, E. *SCHAKAL 97*; Universität Freiburg: Freiburg, Germany, 1997.
(31) Brandenburg, K. *DIAMOND*, version 2.1d; Visual Crystal Structure Information System: Bonn, Germany, 2000.
(32) (a) *X-Shape*, version 1.06; Stoe & Cie GmbH: Darmstadt, Germany, 1999. (b) *X-RED32*, version 1.01; Stoe & Cie GmbH: Darmstadt, Germany, 2001.
(33) Noodleman, L. *J. Chem. Phys.* **1981**, *74*, 5737–5743.
(34) Yamaguchi, K.; Fukui, H.; Fueno, T. *Chem. Lett.* **1986**, *15*, 625–628.
(35) Nishino, M.; Yamanaka, S.; Yoshioka, Y.; Yamaguchi, K. *J. Phys Chem A* **1997**, *101*, 705–712.
(36) Fink, K. *Chem. Phys.* **2006**, *326*, 297–307.
(37) Ahlrichs, R.; Bär, M.; Häser, M.; Horn, H.; Kölmel, C. *Chem. Phys. Lett.* **1989**, *162*, 165–169.
(38) Treutler, O.; Ahlrichs, R. *J. Chem. Phys.* **1995**, *102*, 346–354.
(39) Bauernschmitt, R.; Ahlrichs, R. *Chem. Phys. Lett.* **1996**, *256*, 454–464.
(40) Bauernschmitt, R.; Häser, M.; Treutler, O.; Ahlrichs, R. *Chem. Phys. Lett.* **1997**, *264*, 573–578.
(41) Furche, F.; Rappoport, D. Density functional methods for excited states: Equilibrium structure and electronic spectra. *Computational Photochemistry*; Olivucci, M., Ed.; Elsevier: Amsterdam, 2005, pp 93−128; Chapter 3, Vol. 16 of Theoretical Chemistry and Computation.
(42) Becke, A. D. *Phys. Rev. A* **1988**, *38*, 3098–3100.
(43) Perdew, J. P. *Phys. Rev. B* **1986**, *33*, 8822–8824.

and B3LYP.[44,45] It is well-known that BP86 dramatically overestimates magnetic exchange coupling constants, while hybrid functionals perform much better.[46] The following basis sets were used in the DFT calculations: Fe and Cu were always described by a 10 electron MDF pseudopotential and the corresponding basis set.[47] For the Se atoms next to the Fe ions, a def-SV(P) basis[48] was used; for all others, a 28 electron relativistic pseudopotential and the corresponding DZ basis were applied.[49] For the ligand atoms, we used DZ basis sets. In all BP86 calculations, the resolution of the identity method was applied. Universal auxiliary basis sets[50] were used for all atoms.

For model 1, modified CASCI calculations were performed with the Bochum program package.[51,52] A TZVP basis set[53] from the Turbomole catalogue was used and increased by the first f polarization function. For Se, we used the def-SV(P) basis set, and on the Cu atoms, a large core pseudopotential was used with just one semidiffuse s function (0.4). The relaxation energy of E_{rel} = 15.9 eV for the charge transfer configurations in the modified CI calculation was obtained from clusters in which one or two of the Fe(III) ions were substituted by a pseudopotential representing an Al(III) center. Details of this procedure are given in ref 54. The magnetic susceptibilities were simulated with a program from Staemmler et al.[55] using a spin Hamiltonian of the form

$$\check{H}_{HDVV} = -2J\vec{S}_1\vec{S}_2 + \sum_i g_i\mu_B B m_{si} \quad (1)$$

The first term represents the magnetic exchange coupling of the spins of the two Fe(III) ions S_1 and S_2, the second term, the Zeeman interaction of the two Fe ions with the external magnetic field B. The term g_i is the atomic g factor and μ_B is Bohr's magneton. The influence of a paramagnetic susceptibility was included by

$$\chi(T) = (1-p)\chi_{HDVV}(T) + p\frac{C}{T-\Theta_W} \quad (2)$$

where p is the amount of paramagnetic impurity, C the Curie constant, and Θ_W the Weiss temperature.

Acknowledgment. This work was supported by the Forschungszentrum Karlsruhe and the Deutsche Forschungsgemeinschaft (Center for Functional Nanostructures CFN). A. E. thanks Eckhard Bill from MPG Mühlheim for preliminary Mössbauer measurements and Nico Metz and Emma Tröster for their valuable assistance in the practical work.

(44) Lee, C.; Wang, W.; Parr, R. G. *Phys. Rev. B* **1988**, *37*, 785–789.
(45) Becke, A. D. *J. Chem. Phys.* **1993**, *98*, 5648–5652.
(46) Martin, R. L.; Illas, F. *Phys. Rev. Lett.* **1997**, *79*, 1539–1542.
(47) Dolg, M.; Wedig, U.; Stoll, H.; Preuss, H. *J. Chem. Phys.* **1987**, *86*, 866–872.
(48) Schäfer, A.; Horn, H.; Ahlrichs, R. *J. Chem. Phys.* **1992**, *97*, 2571–2577.
(49) Hurley, M. M.; Pacios, L. F.; Christiansen, P. A. *J. Chem. Phys.* **1986**, *84*, 6840–6853.
(50) Weigend, F. *Phys. Chem. Chem. Phys.* **2006**, *8*, 1057–1065.
(51) Staemmler, V. *Theoret. Chim. Acta* **1977**, *45*, 89–94.
(52) Meier, U.; Staemmler, V. *Theor. Chim. Acta* **1989**, *76*, 95–111.
(53) Schäfer, A.; Huber, C.; Ahlrichs, R. *J. Chem. Phys.* **1994**, *100*, 5829–5835.
(54) Hübner, O.; Fink, K.; Klopper, W. *Phys. Chem. Chem. Phys.* **2007**, *9*, 1911–1920.
(55) Chaudhuri, P.; Birkelbach, F.; Winter, M.; Staemmler, V.; Fleischhauer, P.; Hasse, W.; Flörke, U.; Haupt, H.-J. *J. Chem. Soc., Dalton Trans.* **1994**, 2313–2319.